

Comprehensive Review on High Hydrogen Permselectivity of Palladium Based Membranes: Part I

Research progress of concentration polarisation phenomena

Hasan Mohd Faizal**

Automotive Development Centre, School of Mechanical Engineering, Faculty of Engineering, Universiti Teknologi Malaysia, 81310 UTM Johor Bahru, Johor, Malaysia; School of Mechanical Engineering, Faculty of Engineering, Universiti Teknologi Malaysia, 81310 UTM Johor Bahru, Johor, Malaysia

Bemgba B. Nyakuma

School of Chemical and Energy Engineering, Faculty of Engineering, Universiti Teknologi Malaysia, 81310 Skudai, Johor Bahru, Malaysia

Mohd Rosdzimin Abdul Rahman*

Department of Mechanical Engineering, Faculty of Engineering, Universiti Pertahanan Nasional Malaysia, Kem Sg. Besi, 57000, Kuala Lumpur, Malaysia

Md. Mizanur Rahman, N. B. Kamaruzaman, S. Syahrullail

School of Mechanical Engineering, Faculty of Engineering, Universiti Teknologi Malaysia, 81310 UTM Johor Bahru, Johor, Malaysia

Email: *rosdzimin@gmail.com;
**mfaizal@mail.fkm.utm.my

Palladium based membranes are widely used for supplying ultra-high purity hydrogen to a polymer electrolyte fuel cell (PEFC) installed on small vehicles and various electronic devices. Compared to pressure swing adsorption (PSA), the use of palladium based membrane is more economical for small size (small capacity) applications. The transportation of hydrogen

through a palladium based membrane is governed by Sieverts' Law and quantified with Fick's First Law. Since the 20th century, the fabrication of high-performance palladium based membrane for enhanced hydrogen recovery performance has become practical. However, along with the improvement in hydrogen recovery performance, concentration polarisation becomes unavoidable because hydrogen permeation flux starts to affect hydrogen concentration at the membrane surface. Various parametric studies have investigated the effects of membrane thickness, hydrogen molar fraction and total upstream and downstream pressures on concentration polarisation level. The influence of membrane temperature, permeability, type and number of species in the hydrogen mixture, diffusivity of the hydrogen mixture, system configurations and flow patterns are also reported and comprehensively reviewed in this paper. Part II will complete the presentation.

1. Introduction and Background

Hydrogen purification by palladium-based membrane is one of the most well-known techniques for supplying high purity hydrogen to low temperature operated (1) PEFC in various electronic devices such as tablets, laptop computers and small vehicles. The compact methanol steam reformer that consists of a catalytic burner, reformer and hydrogen purification device in a single package was developed almost two decades ago (2). Over the years, various integrated systems, operating conditions and geometries have been investigated to obtain the optimum operating conditions for reliable performance (3–9). As a result, the compact

reformer has several advantages (i.e. simple and compact) compared to complex systems with separated units (10).

Due to the difficulty and high risk of exposure to accidents, the transportation and storage of gaseous hydrogen are undesirable. Alternatively, the utilisation of alcohols is more practical due to their existence in a liquid form at ambient conditions. Methanol for instance has a relatively high hydrogen:carbon ratio and moderate reaction temperature compared to other alcohols (10, 11). Based on the two step equations of methanol steam reforming, the reaction between vaporised methanol and steam produces hydrogen and carbon dioxide along with carbon monoxide. However, the concentration of carbon monoxide in the electrode of PEFC must be equal to or less than 10 ppm (12). Otherwise, the carbon monoxide could deteriorate the electrode performance by reducing the active surface area for reaction and lowering the partial pressure of hydrogen (13–15).

Hydrogen purification by palladium based membrane is preferable rather than selective carbon monoxide methanation and selective carbon monoxide oxidation (16), in which very high purity of hydrogen and very high permeation flux can be obtained (17–19). PSA is an alternative technique to produce very high purity hydrogen (20). However, the high costs of installing PSA is not economical for small size (or small capacity) applications (21). In addition to the well-known inhibitive carbon monoxide produced from the aforementioned methanol steam reforming, carbon dioxide and excessive methanol from the same reaction (22), hydrogen sulfide (23, 24) and trace amounts of ammonia (20, 25) from coal gasification process, dehydrogenated methanol and ethanol (26) also affect adversely the performance of palladium membranes through its inhibitive mechanism.

Alloying palladium with other metals such as silver and copper is necessary during membrane fabrication to prevent embrittlement when the membrane is used under hydrogen atmosphere and below 573 K and 2 MPa (10). It was found that the maximum amount of permeated hydrogen is obtained when the silver content is 23% (27). In addition, the palladium/silver membrane shows better performance compared to the palladium/copper membrane from the viewpoint of hydrogen permeability. Consequently, there is growing interest in the palladium/silver membrane. In addition to these two types of alloys, the palladium-yttrium membrane has also been previously examined due to its superior hydrogen

permeability. However, this type of membrane is not commercialised due to the expensive processes required to convert the palladium-yttrium alloy into the functional separation membrane (28).

Hydrogen permeation through palladium based membranes is based on the solution-diffusion mechanism (29). When a membrane with sufficient thickness is operated at sufficiently high temperature, the diffusion of hydrogen atoms through the metallic lattice becomes dominant, thus permeation flux can be estimated accurately by using Sieverts' Law (30, 31) that is quantified in Fick's First Law as follows, Equation (i):

$$f = \frac{q}{d} (\sqrt{P_{H_2,1}} - \sqrt{P_{H_2,2}}) \quad (i)$$

where f is the hydrogen permeation mole flux, q is the hydrogen permeance coefficient, d is the membrane thickness, $P_{H_2,1}$ is the hydrogen partial pressure at membrane surface of upstream (or retentate) side and $P_{H_2,2}$ is the hydrogen partial pressure at membrane surface of downstream (or permeate) side. The Sieverts' equation as shown by Equation (i) states that hydrogen permeation is governed by the difference in the square root of the hydrogen partial pressure between the upstream and downstream side.

Membrane temperature (22, 32) and membrane thickness (33–35) are among the important parameters that determine compliance with Sieverts' Law. When the temperature of the membrane is sufficiently high, the adsorption and dissociation of hydrogen atoms at the membrane surface are very fast. Therefore, the diffusion of hydrogen atoms through the metallic lattice becomes a controlling step for permeation. In this case, the hydrogen permeation flux is found to be linear with respect to the difference in the square root of hydrogen partial pressures between the upstream and downstream side. For the case of the palladium/copper membrane, Ma found that Sieverts' Law is valid only when the membrane temperature is set above 573 K (32), whereas for the palladium/silver membrane, the law can be applied even if the temperature is lower than 500 K (22).

The different findings by several groups of researchers had proven that there is no exact value of thickness that can be set as a limit for compliance with Sieverts' Law. Ward and Dao (33) and Federico *et al.* (34) found that the membrane thickness should be higher than 10 μm in order to apply the Sieverts' equation (Equation (i)). Other research groups discovered that the Sieverts' Law

is still valid even though the membrane thickness is below 10 μm (22, 35). These contrary findings are supposed to be caused by difficulty in quantifying various uncontrolled factors such as surface processes (36), surface poisoning (37) and grain boundaries (38).

For the case of pure hydrogen, hydrogen permeation is found to follow the correlation of Sieverts' equation regardless of feed flow rate. However, for mixtures, when the feed flow rate of hydrogen becomes sufficiently high, the hydrogen permeation ratio (fraction of fed hydrogen that permeates membrane) (39) becomes low. Therefore, the hydrogen permeation flux can be predicted accurately by Sieverts' equation (Equation (i)). Further, the term $P_{H_2,1}$ in Equation (i) can be predicted from the bulk value of hydrogen mole fraction at the upstream side, which indicates that hydrogen partial pressures at the membrane surface and the bulk flow are uniform, as illustrated by Line 1 in **Figure 1**.

When a mixture of hydrogen with relatively low feed flow rate (or high permeation ratio) is used, the direct substitution of inlet hydrogen partial pressure ($P_{H_2,in}$) value into the Sieverts' equation causes an overestimation of $P_{H_2,1}$ from the actual permeation flux. This indicates there is a nonuniformity of hydrogen mole fraction in the boundary layer near to membrane surface, as illustrated by Line 2 in **Figure 1**. In this case, several research groups (39–41) mentioned that the hydrogen permeation flux could start to affect the hydrogen concentration at the membrane

surface, thus could trigger the phenomenon of concentration polarisation.

The concentration polarisation phenomenon causes the accumulation of the less permeable species and the depletion of the more permeable species in the boundary layer adjacent to the membrane, thus generating a concentration gradient in the boundary layer (42). Therefore, in such situation, an additional elementary step is essential for the solution-diffusion mechanism of the membrane. This involves the transportation of molecular hydrogen from (to) the bulk gas phase to (from) the gas layer adjacent to the surface at the upstream (downstream) side (33). As a consequence, if the inlet hydrogen partial pressure is directly substituted into the Sieverts' equation (Equation (i)), the hydrogen partial pressure at the membrane surface of upstream side is overestimated, which causes a significant deviation from the actual permeation flux. Chen *et al.* observed that such deviation implies the level of concentration polarisation for a palladium based membrane (41). Based on the analytical study for multicomponent hydrogen mixtures, Caravella *et al.* confirmed that such deviation is caused by the effect of multicomponent external mass transfer (such as concentration polarisation) in addition to non-ideal diffusion through the membrane (43).

Technological advances in membrane materials, modification and fabrication (42) since the end of the 20th century have stimulated the fabrication of very thin membranes in order to substantially improve the permeation performance. Therefore, the phenomenon of concentration polarisation could not be avoided due to the use of membranes with minimal thickness. However, some researchers (44) have recommended installation of baffles in the membrane reactor to decrease the polarisation effect. For palladium based membranes, concentration polarisation has been extensively investigated in the past decade (40) although concentration polarisation had been investigated in the 1990s for separation of a gas-vapour mixture (45). Therefore, significant research interest in the theoretical understanding of the phenomenon has resulted in numerous methods for estimating hydrogen flux for such conditions.

Therefore, a comprehensive review of the transport phenomena for palladium based membranes is performed, particularly on concentration polarisation. In addition to the background of the scenario related to palladium based membranes already highlighted, current information on various

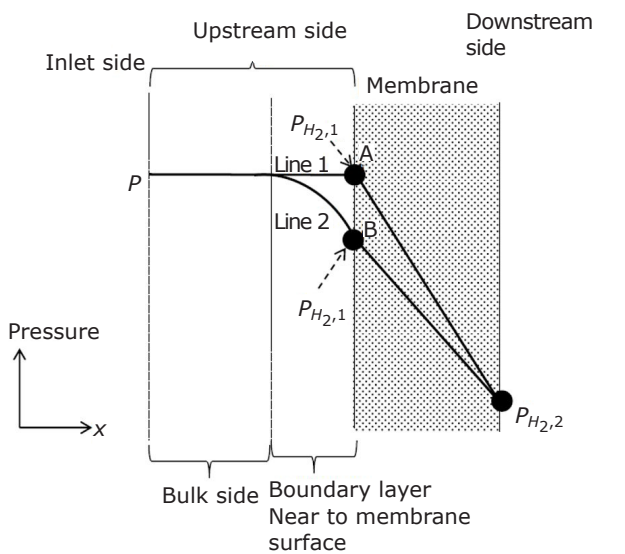


Fig. 1. Schematic diagram of hydrogen partial pressure profile

parametric studies and theoretical approaches for predicting hydrogen permeation flux under the influence of concentration polarisation are covered. Therefore, this review presents critical scientific knowledge and current research on concentration polarisation. The coverage of the present review is significantly different from the published works of Adhikari and Fernando (46), Rei (47), Gallucci *et al.* (21), Al-Mufachi *et al.* (28), Li *et al.* (48), Conde *et al.* (49) and Peters and Caravella (50). Adhikari and Fernando comprehensively reviewed the classification of hydrogen purification membranes, along with the advantages and disadvantages of each type of membrane (46). The study emphasised the superior quality of palladium based membranes in producing ultra-high purity hydrogen due to very high selectivity (46). Similarly, Rei (47) reviewed the advances in permeation through palladium based membranes for the case of a hydrogen mixture based on case studies in Taiwan. Several discoveries on new phenomena of hydrogen permeation such as perturbation of hydrogen permeation due to palladium lattice expansion and hydrogen spillover in the membrane reactor have been described (47). Gallucci *et al.* also highlighted the problem of concentration polarisation in the membrane reactor, although this was not the main topic of the study (21). The authors mainly focused on the route of commercialisation and application of various types of membranes (21). The review of several palladium alloy membranes was presented by Al-Mufachi *et al.* (28). The paper highlighted the advantages and disadvantages of each type of membrane in terms of hydrogen permeability, tensile strength and fabrication costs (28). Subsequently, Li *et al.* reviewed the thermal and chemical stability of palladium based membranes which are considered the two most critical issues for the commercialisation of the membranes (48). In 2017, a review on palladium based membranes was performed by Conde *et al.* (49). The paper presented a review of the alloying elements for palladium based membranes and their effect on the membrane properties. Finally, a most recent overview by Peters and Caravella (50) has covered the scopes of manufacturing process of palladium membranes, membrane materials, membrane modules and reactor design, as well as applications of palladium based membranes.

Based on these published review articles, it can be said that the subject of transport phenomena, particularly on the concentration polarisation, is the novelty for the present review. This paper presents coverage of recent research features

and technological advances on the transport phenomena of palladium based membranes. It also presents the various prediction methods applicable to hydrogen permeation under the influence of concentration polarisation that could serve as a future reference for researchers and industrial practitioners.

2. Factors Affecting Concentration Polarisation in Palladium Based Membranes

In this section, a review of case studies on concentration polarisation is presented. The various studies and types of membrane used for each study are presented in **Table I**, whereas the parameters considered for studying such phenomena are listed in **Table II**. Based on **Table I**, it is evident that most common membranes are tubular, as illustrated by the various configurations in **Figures 2(a)–2(c)**. The studies by Faizal *et al.* (55, 60) examined the phenomenon of concentration polarisation for flat sheet type membranes, which are widely used in compact reformers for hydrogen production (4–5, 65–66). The common configuration for a flat sheet type membrane is illustrated by **Figure 2(d)**. It is interesting to note that various configurations and fluid flow conditions have been considered for studying concentration polarisation. Based on **Table II**, it is evident that the most common varied parameters for concentration polarisation are operating pressure, hydrogen mixture composition, feed flow rate and Reynolds number as well as membrane temperature. However, several studies have focused on geometry improvement to suppress concentration polarisation, as elaborated in this section.

In the early 21st century, Hou and Hughes were among the earliest groups who observed the concentration polarisation during an experiment involving hydrogen permeation with a palladium based membrane (67). The authors confirmed the existence of the concentration polarisation phenomenon during their experiment for a membrane with a thickness of 5 μm to 6 μm . However, the effect was not severe due to the relatively high feed gas velocity, which was a 5% decrease in hydrogen concentration for the various mixing ratios of the binary mixture of hydrogen and nitrogen (67).

Zhang *et al.* (51) were one of the pioneer groups who comprehensively investigated the concentration polarisation phenomenon specifically for palladium based membranes. The

Table I Types of Study and Membranes Used for Investigation on Concentration Polarisation Phenomena

No.	References	Type of study for concentration polarisation	Membrane	
			Type	Thickness ^a , μm
1.	Zhang <i>et al.</i> (51)	Experiment and modelling	Porous ceramic tube supported palladium membrane	–
2.	Pizzi <i>et al.</i> (52)	Experiment and analytical	Palladium/20 wt% silver tubular membranes deposited on ceramic supports	2.5
3.	Catalano <i>et al.</i> (40)	Experiment and analytical	Palladium/20 wt% silver tubular membrane with ceramic support	2.5
4.	Caravella <i>et al.</i> (53)	Modelling and analytical	Tubular type self-supported palladium based membrane	1–150
5.	Coroneo <i>et al.</i> (44)	Simulation and experiment	Tubular palladium/silver membrane deposited on tube	3
6.	Caravella <i>et al.</i> (54)	Modelling and analytical	Self-supported tubular palladium based membrane	60
7.	Chen <i>et al.</i> (39)	Numerical simulation	Self-supported tubular type palladium based membrane	–
8.	Chen <i>et al.</i> (41)	Numerical simulation	Self-supported tubular type palladium based membrane	–
9.	Faizal <i>et al.</i> (55)	Experiment and analytical	Self-supported circular flat sheet type palladium/23 wt% silver membrane	25
10.	Chen <i>et al.</i> (56)	Numerical simulation	Self-supported tubular palladium membrane	–
11.	Chen <i>et al.</i> (57)	Experiment	Palladium and palladium/copper membrane with porous stainless steel support	6.5–7.0
12.	Chen <i>et al.</i> (58)	Numerical simulation	Self-supported tubular palladium membrane	–
13.	Nekhamkina and Sheintuch (59)	Analytical	Self-supported tubular palladium membrane	–
14.	Zhao <i>et al.</i> (23)	Experiment	Palladium/copper tubular membrane with ceramic substrate	5
15.	Faizal <i>et al.</i> (60)	Experiment and analytical	Self-supported circular flat sheet type palladium/23 wt% silver membrane	25
16.	Nakajima <i>et al.</i> (61)	Experiment and numerical	Tubular palladium/silver membrane with ceramic support	–
17.	Caravella and Sun (62)	Analytical and simulation (for case study of water-gas shift reaction)	Self-supported tubular palladium based membrane	–
18.	Kian <i>et al.</i> (63)	Experiment	Palladium layer deposited on yttria stabilised zirconia (YSZ) support (tubular)	11
			Palladium/gold layer deposited on YSZ deposited on Al ₂ O ₃ substrate (tubular)	8
19.	Helmi <i>et al.</i> (64)	Simulation and experiment	Pd _{0.85} Ag _{0.15} based tubular membrane supported on Al ₂ O ₃ porous in fluidised membrane reactor	4.5

^a Sign – indicates not available

effect of various parameters such as pressure, temperature, feed gas flow rate and permeability was investigated experimentally. Also, the parameters were interpreted through mathematical

modelling particularly for tubular membranes with porous ceramic supports. The authors found that when the feed gas flow rate is increased, the concentration polarisation is weakened, resulting

Table II Varied Parameters for Studying the Effect on Concentration Polarisation

Reference	Parameters
Zhang et al. (51)	Feed flow rate: $0-5.1 \times 10^{-5} \text{ m}^3 \text{ s}^{-1}$. Pressure: 101.3–405.3 kPa (difference in total pressure). Temperature: 623–773 K
Pizzi et al. (52)	Pressure: 20–600 kPa (difference in total pressure). Inlet H_2 concentration: 88 vol% and 50 vol%
Catalano et al. (40)	Feed flow rate ($\text{m}^3 \text{ s}^{-1}$): $(1.67-5.00) \times 10^{-5} \text{ m}^3 \text{ s}^{-1}$ (at normal condition). Pressure: up to 600 kPa (difference in total pressure). Inlet H_2 concentration: 50 vol% and 88 vol%. Temperature: 673–773 K. Binary ($\text{H}_2:\text{N}_2$, $\text{H}_2:\text{CH}_4$) and ternary mixtures ($\text{H}_2:\text{N}_2:\text{CH}_4$)
Caravella et al. (53)	Membrane thickness: 1–150 μm . Permeance: $0.1-20 \text{ mmol m}^{-2} \text{ s}^{-1} \text{ Pa}^{-0.5}$. Reynolds Number: 2100–8000. Upstream total pressure: 200–1000 kPa. Downstream total pressure: 100–800 kPa. Inlet H_2 concentration: 0–1 molar fraction. Temperature: 573–773 K
Coroneo et al. (44)	0, 2 and 3 (number of baffles)
Caravella et al. (54)	Total upstream pressure: 400–1000 kPa. CO partial pressure: 0–1000 kPa. Inlet H_2 concentration: 0–1 molar fraction. Ternary ($\text{H}_2:\text{CO}:\text{N}_2$) and binary mixture ($\text{H}_2:\text{CO}$)
Chen et al. (39)	Permeance: $10^{-3}-1 \text{ mmol m}^{-2} \text{ s}^{-1} \text{ Pa}^{-0.5}$. Reynolds number: 20–2000. Pressure: 506.5–3039 kPa. Inlet H_2 concentration: 0.20–0.80 molar fraction
Chen et al. (41)	Feed flow rate: $2.713 \times 10^{-4}-4.3408 \times 10^{-3} \text{ mol s}^{-1}$. Reynolds number: 10–50 (retentate side) and 2–2000 (permeate side). Flow pattern: countercurrent and cocurrent modes. Position of the feed flow: in lumen or shell side
Faizal et al. (55)	Feed flow rate: $1.489 \times 10^{-5}-2.976 \times 10^{-4} \text{ mol s}^{-1}$. Upstream total pressure: 200–300 kPa
Chen et al. (56)	Reynolds number: 20–2000 (permeate side) and 20–800 (retentate). Pressure difference: 506.5–3039 kPa. Shell diameter: 25–100 mm
Chen et al. (57)	Feed flow rate: $1.67-3.33 \times 10^{-6} \text{ m}^3 \text{ s}^{-1}$. Pressure: 50.7–405.2 kPa (H_2 partial pressure difference). Inlet H_2 concentration: 50–100 vol%
Chen et al. (58)	Baffle patterns, positions at shell wall, ratio of baffle length to radius (0–0.75)
Nekhamkina and Sheintuch (59)	Pressure: $31.62-632.46 \text{ Pa}^{0.5}$ (initial driving force). Inlet H_2 concentration: 0.50–0.88 (molar fraction). Separation parameter, $\Gamma (<29)$
Zhao et al. (23)	Feed flow rate: $4.17 \times 10^{-6}-4.00 \times 10^{-3} \text{ m}^3 \text{ s}^{-1}$. Inlet H_2 concentration: 0.50–0.90 (molar fraction). Temperature: 673–773 K. H_2S concentration: 7–35 ppm
Faizal et al. (60)	Feed flow rate: $2.78 \times 10^{-5}-2.50 \times 10^{-4} \text{ mol s}^{-1}$. Inlet H_2 concentration: 0.70–0.80 (molar fraction). Various species in H_2 mixture ($\text{H}_2:\text{N}_2$, $\text{H}_2:\text{Ar}$, $\text{H}_2:\text{He}$ and $\text{H}_2:\text{CO}_2$)
Nakajima et al. (61)	Feed flow rate: $5.0 \times 10^{-4}-1.5 \times 10^{-3} \text{ Nm}^3 \text{ s}^{-1} \text{ m}^{-2}$. Internal diameter of reactor vessel: $1.66-2.39 \times 10^{-2} \text{ m}$
Kian et al. (63)	Total upstream pressure: 150–600 kPa. Various ternary and quaternary mixtures as well as a senary mixture $\rightarrow \text{H}_2:\text{Ar}$, $\text{H}_2:\text{He}$, $\text{H}_2:\text{CH}_4$, $\text{H}_2:\text{H}_2\text{O}$, $\text{H}_2:\text{CO}:\text{He}$ (example of ternary mixture), $\text{H}_2:\text{CO}_2:\text{CO}:\text{He}$ (example of quaternary mixture), $\text{H}_2:\text{CO}_2:\text{H}_2\text{O}:\text{CH}_4:\text{CO}:\text{He}$. Gas hourly space velocity (GHSV): 221–882 h^{-1} . Flow rates: 276–1078 ml min^{-1}
Helmi et al. (64)	Relative fluidisation velocity: 1.3–3.3. H_2 mole fraction: 0.1, 0.25 and 0.45

in higher hydrogen permeation. For instance, for the case of membrane temperature of 723 K, when the feed flow rate was 5 ml s^{-1} (equivalent to $5 \times 10^{-6} \text{ m}^3 \text{ s}^{-1}$), the concentration polarisation degree for hydrogen (ratio of hydrogen permeation flux with concentration polarisation to hydrogen permeation flux without concentration) was around 0.54. However, when the feed flow rate was increased to around 14 ml s^{-1} (equivalent to $14 \times 10^{-6} \text{ m}^3 \text{ s}^{-1}$), the concentration polarisation degree for hydrogen became 1, that is no effect of concentration polarisation on hydrogen permeation flux was found. Furthermore, the authors reported

that the observed phenomena are mainly due to the higher removal rate of accumulated nitrogen in the boundary layer at higher feed flow rates (51). However, an increase in pressure at the retentate or upstream side (at constant permeated pressure) increases concentration polarisation, as clearly described by the mathematical modelling developed in the study. Based on their study, at constant temperature of 723 K, for the case of pressure of 2 atm (equivalent to 202.6 kPa), the concentration polarisation degree for hydrogen already reached a value of 1 (no effect of concentration polarisation) when the feed flow rate was around 14 ml s^{-1}

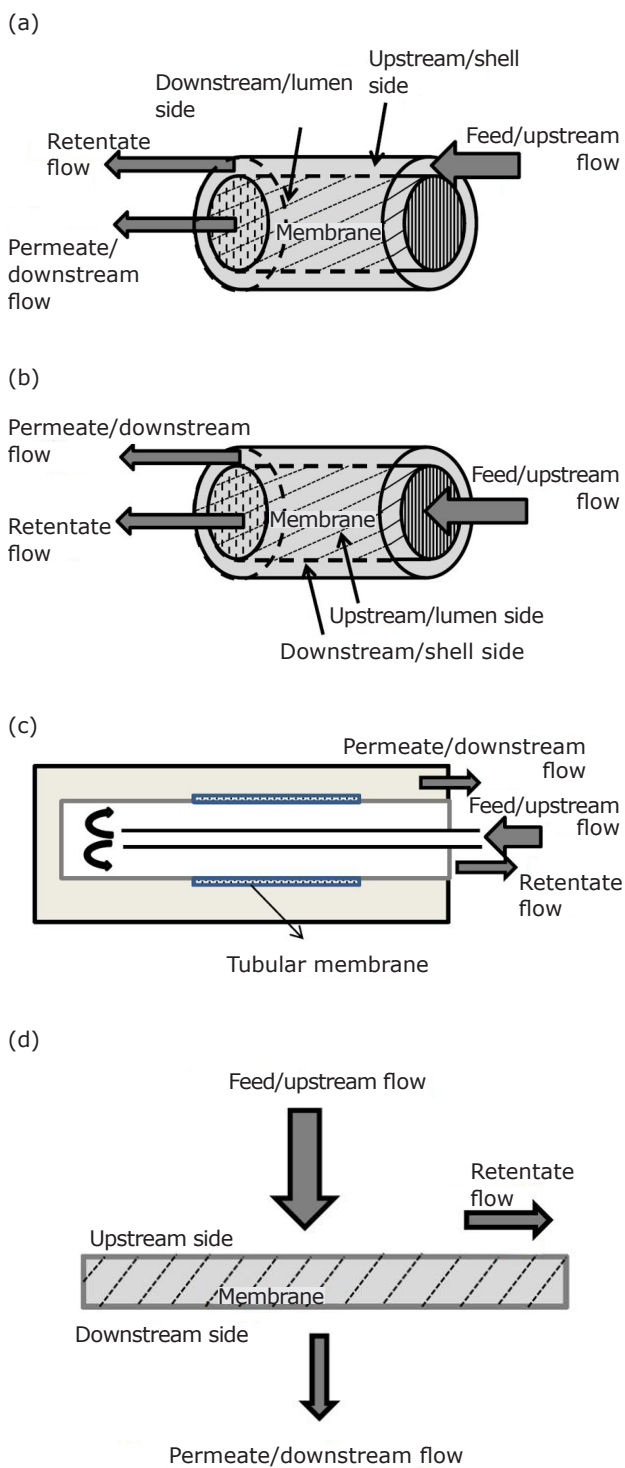


Fig. 2. (a) Tubular type membrane configuration (feed flow is issued through shell side); (b) tubular type membrane configuration (feed flow is issued through lumen side); (c) tubular type membrane with 'finger-like' configuration (front view); (d) circular flat sheet type membrane configuration (front view)

(equivalent to $14 \times 10^{-6} \text{ m}^3 \text{ s}^{-1}$). However, for the case of higher pressure of 4 atm (equivalent to 405.2 kPa), the concentration polarisation

degree for hydrogen still not reached value of 1 even though feed flow rate was increased to 32 ml s^{-1} (equivalent to $32 \times 10^{-6} \text{ m}^3 \text{ s}^{-1}$). Based on the model, the observed trend is related to the proportional relation between the mass transfer coefficient of the retentate side and the diffusion coefficient, which is reciprocal to operating pressure (51). Therefore, the findings of Zhang *et al.* corroborated the previous findings by Morguez and Sanchez (68), which reported that the effect of selectivity is less significant compared to feed gas flow rate, pressure and permeability (68). The authors also observed that the temperature range used in their experiment did not trigger the concentration polarisation phenomenon. However, the authors did not rule out the possibility of concentration polarisation when the hydrogen permeation rate is enhanced due to the increase in temperature (51).

Pizzi *et al.* performed an experimental study for ultra-thin ($\sim 2.5 \text{ }\mu\text{m}$ thickness) palladium/silver membranes deposited on ceramic supports. The authors observed that pronounced concentration polarisation occurred regardless of the composition mixture (52). As a result, the phenomenon was evident despite the concentration of nitrogen in a binary mixture of $\text{H}_2:\text{N}_2$ being relatively very low (12 vol%) (52). For this case, it was found that when Sieverts' driving force is set to $0.8 \text{ bar}^{0.5}$ (equivalent to $253 \text{ Pa}^{0.5}$), the hydrogen permeate flux is only $0.26 \text{ mol s}^{-1} \text{ m}^{-2}$, that is significantly lower if compared to the permeate flux obtained when the concentration polarisation effect is negligible (permeate flux of $0.68 \text{ mol s}^{-1} \text{ m}^{-2}$).

The lack of extensive studies on the detailed mechanism of concentration polarisation specifically for palladium based membranes prompted Catalano *et al.* (40) to explore this research area. The findings of Catalano *et al.* demonstrated a similar trend with that of Zhang *et al.* (51) in terms of the effect of feed flow rate, and Pizzi *et al.* (52) in terms of the effect of mixture composition on the concentration polarisation phenomena. Compared to previous research, a fundamental investigation on the ternary mixture of $\text{H}_2:\text{N}_2:\text{CH}_4$ (volume ratio of 50:25:25) was also conducted for the first time. The findings showed that the permeation flux was marginally less than the flux for the binary mixture of $\text{H}_2:\text{N}_2$ (volume ratio of 50:50) but almost similar to the $\text{H}_2:\text{CH}_4$ (volume ratio of 50:50) mixture. Therefore, the findings reveal that there was a very slight decrease in permeation flux, which occurred when nitrogen was replaced with methane (40). In this case, previous researchers have confirmed that the inhibitive effect caused by methane is very

minimal, thus can be neglected (69). Based on the findings of Catalano *et al.* (40) and Jung *et al.* (69), it is evident that the severity level of concentration polarisation is independent on number of species (binary or ternary) in the non-inhibitive hydrogen mixture. Catalano *et al.* also have interpreted the level of concentration polarisation for various operating conditions using a dimensionless polarisation number, which is defined as the ratio of gas phase to membrane sensitivity factor (40). The polarisation number of much higher than 1 ($S \gg 1$) means concentration polarisation is dominant, whereas when the number is much less than 1 ($S \ll 1$), resistance by the metal membrane controls the entire permeation process. The authors discovered that for both cases of ternary and binary hydrogen mixtures with feed flow rates of 1 NI min^{-1} to 3 NI min^{-1} and relatively low inlet hydrogen concentration (50 vol% H_2), the concentration polarisation becomes dominant, that is $S \gg 1$. However the value of S is reduced when hydrogen concentration or feed flow rate is increased. As example, for the case of binary mixture of $\text{H}_2:\text{N}_2$ (50 vol% H_2 and 50 vol% N_2) with operating temperature and total pressure of 673 K and 600 kPa, respectively, when the feed flow rate was increased from 1 NI min^{-1} to 3 NI min^{-1} , S reduced significantly from 6 to 2.5.

Most of the studies on concentration polarisation elaborated previously used palladium based membrane with support that influences the hydrogen permeation process (70). Conversely, Caravella *et al.* (53) examined the concentration polarisation phenomenon on self-supported palladium-based membrane in which case the effect of support was eliminated. In addition to the previous studies, other researchers (40, 51–52), have analysed the broader range of upstream hydrogen molar fraction, total upstream pressure, downstream total pressure, operating membrane temperature, membrane thickness and permeability to develop polarisation maps as a very useful guide for membrane reactor designer. The term concentration polarisation coefficient (CPC) was introduced in the maps as a demonstration for the level of concentration polarisation. Here, when the value of CPC is 0, it means no polarisation occurs while the value of 1 indicates the occurrence of total or maximum polarisation. Additional parameters were considered in this study that were not covered by the other previous researchers, namely: operating temperature, permeance, total downstream pressure and membrane thickness. Furthermore, the analysis demonstrated that the

severity of concentration polarisation increases when the temperature and permeance are increased whereas the total downstream pressure and membrane thickness are reduced (53). As example, when Reynolds number, hydrogen retentate molar fraction, temperature, pressure at retentate side and pressure at permeate side were set to 2100, 0.40, 500°C, 1000 kPa and 200 kPa, respectively, the CPC increased significantly from around 0.13 to around 0.65 (thus concentration polarisation effect become stronger) when membrane thickness was reduced from 50 μm to 5 μm . Similar to the assertion by Morgues *et al.* (68), Caravella *et al.* (53) also found that the hydrogen flux itself plays a significant role during concentration polarisation.

Caravella *et al.* extended their analytical study to cover the concentration polarisation phenomena for a hydrogen mixture that contains well-known inhibitive species of carbon monoxide (22, 71–76). In this study (54), the authors simultaneously considered the effects of concentration polarisation and inhibition by carbon monoxide by merging their previously introduced approach (53) and the approach by Barbieri *et al.* (77). Similar to their previous study (53), the authors introduced a parameter so-called permeation reduction coefficient (PRC) that includes both polarisation and carbon monoxide inhibitive effects simultaneously. Interestingly, it was found that when the polarisation and carbon monoxide inhibition occur at the same time, the hydrogen permeation flux obtained is lower compared to the flux obtained when both phenomena occurred separately. This is mainly due to the polarisation of the inhibitor carbon monoxide toward the membrane surface, which increases the carbon monoxide partial pressure at the surface (54). The researchers found that for binary mixture of hydrogen and carbon monoxide, when operating temperature, membrane thickness, Reynolds number, hydrogen upstream molar fraction, total upstream pressure and downstream pressure are set to approximately 647 K, 60 μm , 1200, 0.60, 1000 kPa and 200 kPa, respectively, the permeating flux for the cases of polarisation only, inhibition by carbon monoxide only, and simultaneous polarisation and inhibition are around 85 $\text{mmol m}^{-2} \text{s}^{-1}$, 71.5 $\text{mmol m}^{-2} \text{s}^{-1}$ and 67 $\text{mmol m}^{-2} \text{s}^{-1}$ (54). The inhibition of carbon monoxide under the influence of concentration polarisation is expected since the low feed flow rate is generally applied, for instance, during steam reforming for application in small portable electrical devices (8, 66).

The phenomenon of concentration polarisation was featured by the two-dimensional numerical method for tubular type (39) and flat sheet type (78) membranes. In general, for permeation with tubular type membrane under concentration polarisation influence, the direction of hydrogen concentration decrease for binary mixture of H₂:N₂ is from the region around the leading edge (inlet part) to the tailing edge (outlet part) (39). This phenomenon is featured by **Figure 3**, in which dimensionless hydrogen concentration gradient decreases from the leading edge to the tailing edge of the membrane surface regardless of hydrogen volume percentage. However, for the case with vertical flow towards flat sheet type membrane surface, the hydrogen concentration is highest at the centre of the membrane, and decreases in radial direction, as shown by **Figure 4** (78). These studies investigated the hydrogen concentration distribution around the membrane surface for various important parameters such as operating pressure, hydrogen molar fraction, feed flow rate (or Reynolds number) and membrane permeance. The qualitative simulated results reveal that the hydrogen concentration decreases at the membrane surface due to the effect of hydrogen flux itself during the phenomena. However, the severity level of concentration polarisation for the

various parameters above is generally similar to the values described quantitatively by previous experimental and analytical studies (40, 51–54). Chen *et al.* introduced an important parameter called hydrogen permeation ratio (HPR) to indicate the level of concentration polarisation (39). The HPR is defined as the ratio of hydrogen permeation rate across the membrane to the hydrogen feed rate at the inlet. The authors concluded that a decrease in value of HPR indicates that the severity of concentration polarisation is diminished. As an example, for the case of binary mixture of H₂:N₂ (H₂ mole fraction of 0.50) with pressure difference and membrane permeance of 30 atm and 10⁻⁴ mol m⁻² s⁻¹ Pa^{-0.5}, respectively, HPR decreased from 96 to 3 when Reynolds number was increased from 20 to 2000, thus severity of concentration polarisation is significantly reduced (39). It is interesting to note that when the aforementioned four important parameters (operating pressure, hydrogen molar fraction, feed flow rate and membrane permeance) were set in such a way to cause the effect of concentration polarisation to become very significant, the hydrogen concentration gradient is very high at the leading edge of the membrane (in the region near to the inlet) and then decays faster. Due to this phenomenon, there was almost no driving force for

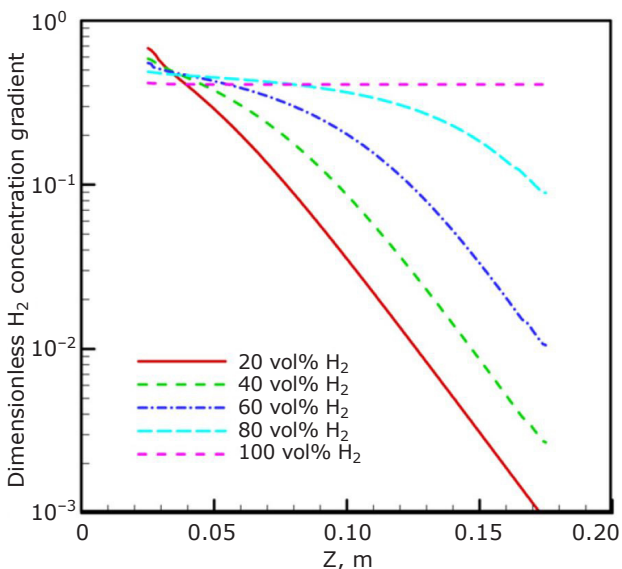


Fig. 3. Dimensionless hydrogen concentration gradient from the leading edge ($Z = 0.025$ m) to the tailing edge ($Z = 0.175$ m) of the membrane surface, for the case of Reynolds number of 200, pressure difference of 30 atm and permeance of 10⁻³ Reprinted from (39) Copyright (2011), with permission from Elsevier

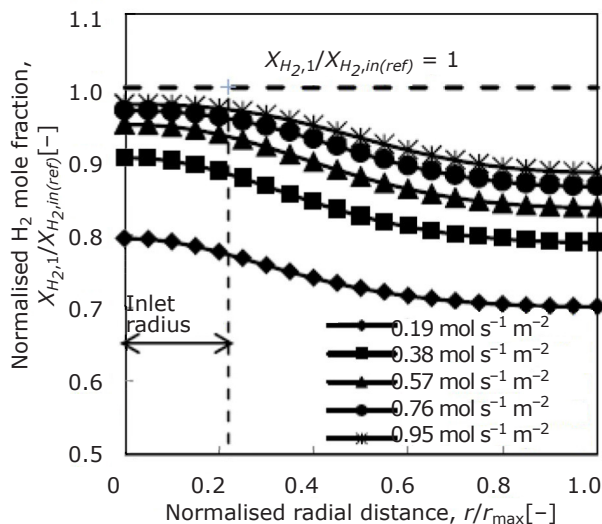


Fig. 4. Radial profile of hydrogen concentration on the membrane surface as a function of mean mole flux (feed flow rate divided by effective membrane surface area) for the case of inlet hydrogen mole fraction of 0.75, membrane temperature of 623 K, total upstream pressure of 0.25 MPa and total downstream pressure of 0.10 MPa (78)

permeation in most of the remaining membrane length, as demonstrated by **Figure 5** (refer to the case of permeance (K) of 10^{-3}) (39). **Figure 5** also demonstrates that when the permeance is increased, the tendency for concentration polarisation to occur increases. Based on Nagy *et al.* (79), a convex shape can be observed for the hydrogen concentration curve in a boundary layer during concentration polarisation phenomena, once the convective flow starts to play a role in the diffusive flow of the layer (80, 81). Based on these numerical simulation studies, Chen *et al.* also asserted that the concentration polarisation phenomenon is not significant when the hydrogen permeation ratio (H_2 permeation rate: H_2 feed rate) is less than 30%. It is important to note that even if the concentration polarisation can be improved (and more hydrogen flux can be obtained), the HPR that indicates hydrogen recovery becomes smaller, and this becomes a shortcoming for the membrane performance (39).

Subsequently, Chen *et al.* extended their numerical simulation to the tubular type membrane with simultaneous use of feed flow and sweep flow (41) under concentration polarisation influence. The advantage of using sweep flow to improve hydrogen permeation flux (and to abate concentration polarisation) has been confirmed by previous researchers (6, 7, 82–84). When the sweep flow rate at the permeated side is increased, the hydrogen partial pressure at the membrane surface of the permeated side can be reduced, thus hydrogen permeation flux increases (and concentration polarisation is weakened) due to increase in hydrogen partial pressure difference (7, 83). For instance, in

the case of countercurrent mode with the use of sweep gas in the shell side (outside tubular membrane and inside shell), the improvement in hydrogen flux was improved by 12.3% when the sweep flow rate was increased from 2.713 mol s^{-1} to $4.3408 \text{ mol s}^{-1}$, thus indicating the importance of sweep flow rate in improving hydrogen flux. In this case, the optimum flow rate of sweep gas can be estimated from the arctangent function (41, 85) of feed gas flow rate, once the flow rate or Reynolds number of the feed gas is specified. Here, the flow rate of sweep gas is considered optimum when the flow rate can give the maximum hydrogen permeation flux and sufficiently high hydrogen recovery (up to 95% H_2 recovery) could be maintained (41). It is interesting to note that the coupling between feed gas and sweep gas will give better separation performance when countercurrent mode is applied (5, 41). It is also interesting to note that whether the feed gas is issued in the lumen side (inside tubular membrane) or the shell side (outside tubular membrane and inside the shell) during countercurrent mode, the difference in hydrogen flux for both configurations is negligible. Therefore, this implies the independence of hydrogen flux on the position of the feed flow. Also, the difference in hydrogen permeation flux between cocurrent mode and countercurrent mode can be reduced by increasing the feed flow rate. Similar to the feed flow rate, a decrease in the sweep flow rate causes the effect of concentration polarisation to become stronger.

Part II (86) continues the discussion and provides the conclusions.

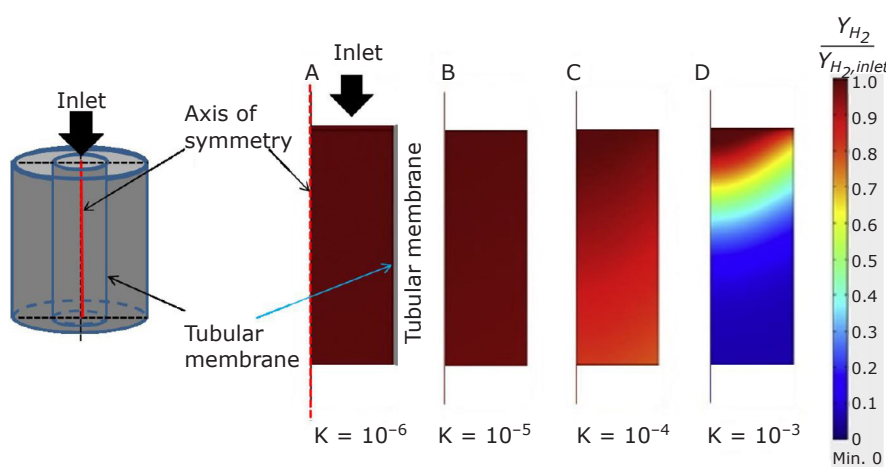


Fig. 5. Distributions of concentration contour for various hydrogen permeance values ($H_2:N_2$ mixture, inlet $H_2 = 50\%$, Reynolds number = 200 and pressure difference = 30 atm). Reprinted from (39) Copyright (2011), with permission from Elsevier

Acknowledgement

The authors acknowledge the Ministry of Higher Education Malaysia and Universiti Teknologi Malaysia for giving cooperation and full support in this research. The authors wish to thank Research Management Centre (RMC) for the Tier 2 Grant (Vote No.: 16J28) from Ministry of Higher Education and Universiti Teknologi Malaysia.

References

- E. Carcadea, H. Ene, D. B. Ingham, R. Lazar, L. Ma, M. Pourkashanian and I. Stefanescu, *Int. Commun. Heat Mass Transf.*, 2005, **32**, (10), 1273
- B. Emonts, J. Bøgild Hansen, S. Løegsgaard Jørgensen, B. Höhlelein and R. Peters, *J. Power Sources*, 1998, **71**, (1–2), 288
- E. Kikuchi, *Catal. Today*, 2000, **56**, (1–3), 97
- B. Arstad, H. Venvik, H. Klette, J. C. Walmsley, W. M. Tucho, R. Holmestad, A. Holmen and R. Bredesen, *Catal. Today*, 2006, **118**, (1–2), 63
- A. Basile, G. Tereschchenko, N. Orekhova, M. M. Ermilova, F. Gallucci and A. Iulianelli, *Int. J. Hydrogen Energy*, 2006, **31**, (12), 1615
- A. Basile, S. Tosti, G. Capannelli, G. Vitulli, A. Iulianelli, F. Gallucci and E. Drioli, *Catal. Today*, 2006, **118**, (1–2), 237
- A. Iulianelli, T. Longo and A. Basile, *Int. J. Hydrogen Energy*, 2008, **33**, (20), 5583
- A. S. Damle, *J. Power Sources*, 2009, **186**, (1), 167
- S. H. Israni and M. P. Harold, *J. Membr. Sci.*, 2011, **369**, (1–2), 375
- V. Gepert, M. Kilgus, T. Schiestel, H. Brunner, G. Eigenberger and C. Merten, *Fuel Cells*, 2006, **6**, (6), 472
- S. Fujimoto, H. Ishihara and S. Tsuruno, *JSME Int. J.*, 1987, **30**, (267), 1437
- K. Kusakabe, *Membrane*, 2005, **30**, (1), 2
- K. Narusawa, M. Hayashida, D. Kurashima, K. Wakabayashi and Y. Kamiya, *JSME Int. J. Ser. B*, 2003, **46**, (4), 643
- K. Narusawa, M. Hayashida, D. Kurashima, K. Murooka, K. Wakabayashi and Y. Kamiya, *Trans. Japan Soc. Mech. Eng. Ser. B*, 2003, **69**, (687), 2553
- J.-Y. Lee, J. Joo, J. K. Lee, S. Uhm, E. S. Lee, J. H. Jang, N.-K. Kim, Y.-C. Lee and J. Lee, *Korean J. Chem. Eng.*, 2010, **27**, (3), 843
- B. Höhlelein, M. Boe, J. Bøgild-Hansen, P. Bröckerhoff, G. Colman, B. Emonts, R. Menzer and E. Riedel, *J. Power Sources*, 1996, **61**, (1–2), 143
- G. J. Grashoff, C. E. Pilkington and C. W. Corti, *Platinum Metals Rev.*, 1983, **27**, (4), 157
- Y.-M. Lin and M.-H. Rei, *Sep. Purif. Technol.*, 2001, **25**, (1–3), 87
- A. Basile, A. Iulianelli, T. Longo, S. Liguori and M. De Falco, 'Pd-Based Selective Membrane State-of-the-Art', in "Membrane Reactors for Hydrogen Production Processes", eds. M. De Falco, L. Marrelli and G. Iaquaniello, Springer-Verlag London Ltd, London, UK, 2011, pp. 21–55
- T. A. Peters, J. M. Polfus, M. Stange, P. Veenstra, A. Nijmeijer and R. Bredesen, *Fuel Process. Technol.*, 2016, **152**, 259
- F. Gallucci, E. Fernandez, P. Corengia and M. van Sint Annaland, *Chem. Eng. Sci.*, 2013, **92**, 40
- S. H. Israni and M. P. Harold, *Ind. Eng. Chem. Res.*, 2010, **49**, (21), 10242
- L. Zhao, A. Goldbach, C. Bao and H. Xu, *J. Membr. Sci.*, 2015, **496**, 301
- C.-H. Chen and Y. H. Ma, *J. Membr. Sci.*, 2010, **362**, (1–2), 535
- J. Zhang, H. Xu and W. Li, *J. Membr. Sci.*, 2006, **277**, (1–2), 85
- H. Dannetun, L. Wilzén and L.-G. Petersson, *Surf. Sci.*, 1996, **357–358**, 804
- S. Uemiyama, N. Sato, H. Ando, Y. Kude, T. Matsuda and E. Kikuchi, *J. Membr. Sci.*, 1991, **56**, (3), 303
- N. A. Al-Mufachi, N. V. Rees and R. Steinberger-Wilkens, *Renew. Sustain. Energy Rev.*, 2015, **47**, 540
- G. L. Holleck, *J. Phys. Chem.*, 1970, **74**, (3), 503
- A. Sieverts and G. Zapf, *Zeit. Phys. Chem.*, 1935, **174**, (1), 359
- R. W. Baker, "Membrane Technology and Applications", 3rd Edn., John Wiley and Sons Ltd, Chichester, UK, 2012, 575 pp
- Y. H. Ma, 'Hydrogen Separation Membranes', in "Advanced Membrane Technology and Applications", eds. N. N. Li, A. G. Fane, W. S. W. Ho and T. Matsuura, John Wiley & Sons Inc, Hoboken, USA, 2008, pp. 671–684
- T. L. Ward and T. Dao, *J. Membr. Sci.*, 1999, **153**, (2), 211
- F. Guazzone, E. E. Engwall and Y. H. Ma, *Catal. Today*, 2006, **118**, (1–2), 24
- S. Uemiyama, T. Matsuda and E. Kikuchi, *J. Membr. Sci.*, 1991, **56**, (3), 315
- J. P. Collins and J. D. Way, *Ind. Eng. Chem. Res.*, 1993, **32**, (12), 3006
- A. B. Antoniazzi, A. A. Haasz and P. C. Stangeby, *J. Nucl. Mater.*, 1989, **162–164**, 1065
- S. Yan, H. Maeda, K. Kusakabe and S. Murooka, *Ind. Eng. Chem. Res.*, 1994, **33**, (3), 616
- W.-H. Chen, W.-Z. Syu and C.-I. Hung, *Int. J. Hydrogen Energy*, 2011, **36**, (22), 14734

40. J. Catalano, M. G. Baschetti and G. C. Sarti, *J. Membr. Sci.*, 2009, **339**, (1–2), 57
41. W.-H. Chen, W.-Z. Syu, C.-I. Hung, Y.-L. Lin and C.-C. Yang, *Int. J. Hydrogen Energy*, 2012, **37**, (17), 12666
42. G. He, Y. Mi, P. L. Yue and G. Chen, *J. Membr. Sci.*, 1999, **153**, (2), 243
43. A. Caravella, S. Hara, E. Drioli and G. Barbieri, *Int. J. Hydrogen Energy*, 2013, **38**, (36), 16229
44. M. Coroneo, G. Montante and A. Paglianti, *Ind. Eng. Chem. Res.*, 2010, **49**, (19), 9300
45. O. Lüdtke, R.-D. Behling and K. Ohlrogge, *J. Membr. Sci.*, 1998, **146**, (2), 145
46. S. Adhikari and S. Fernando, *Ind. Eng. Chem. Res.*, 2006, **45**, (3), 875
47. M. H. Rei, *J. Taiwan Inst. Chem. Eng.*, 2009, **40**, (3), 238
48. H. Li, A. Caravella and H. Y. Xu, *J. Mater. Chem. A*, 2016, **4**, (37), 14069
49. J. J. Conde, M. Maroño and J. M. Sánchez-Hervás, *Sep. Purif. Rev.*, 2017, **46**, (2), 152
50. T. Peters and A. Caravella, *Membranes*, 2019, **9**, (2), 25
51. J. Zhang, D. Liu, M. He, H. Xu and W. Li, *J. Membr. Sci.*, 2006, **274**, (1–2), 83
52. D. Pizzi, R. Worth, M. G. Baschetti, G. C. Sarti and K. Noda, *J. Membr. Sci.*, 2008, **325**, (1), 446
53. A. Caravella, G. Barbieri and E. Drioli, *Sep. Purif. Technol.*, 2009, **66**, (3), 613
54. A. Caravella, F. Scura, G. Barbieri and E. Drioli, *J. Phys. Chem. B*, 2010, **114**, (38), 12264
55. H. M. Faizal, R. Kizu, Y. Kawamura, T. Yokomori and T. Ueda, *J. Therm. Sci. Technol.*, 2013, **8**, (1), 120
56. W.-H. Chen, W.-Z. Syu, C.-I. Hung, Y.-L. Lin and C.-C. Yang, *Int. J. Hydrogen Energy*, 2013, **38**, (2), 1145
57. W.-H. Chen, M.-H. Hsia, Y.-H. Chi, Y.-L. Lin and C.-C. Yang, *Appl. Energy*, 2014, **113**, 41
58. W.-H. Chen, C.-H. Lin and Y.-L. Lin, *J. Membr. Sci.*, 2014, **472**, 45
59. O. Nekhamkina and M. Sheintuch, *Chem. Eng. J.*, 2015, **260**, 835
60. H. M. Faizal, Y. Kawasaki, T. Yokomori and T. Ueda, *Sep. Purif. Technol.*, 2015, **149**, 208
61. T. Nakajima, T. Kume, Y. Ikeda, M. Shiraki, H. Kurokawa, T. Iseki, M. Kajitani, H. Tanaka, H. Hikosaka, Y. Takagi and M. Ito, *Int. J. Hydrogen Energy*, 2015, **40**, (35), 11451
62. A. Caravella and Y. Sun, *Int. J. Hydrogen Energy*, 2016, **41**, (27), 11653
63. K. Kian, C. M. Woodall, J. Wilcox and S. Liguori, *Environments*, 2018, **5**, (12), 128
64. A. Helmi, R. J. W. Voncken, A. J. Raijmakers, I. Roghair, F. Gallucci and M. van Sint Annaland, *Chem. Eng. J.*, 2018, **332**, 464
65. A. Unemoto, A. Kaimai, K. Sato, T. Otake, K. Yashiro, J. Mizusaki, T. Kawada, T. Tsuneki, Y. Shirasaki and I. Yasuda, *Int. J. Hydrogen Energy*, 2007, **32**, (14), 2881
66. H. M. Faizal, M. Kuwabara, R. Kizu, T. Yokomori and T. Ueda, *J. Therm. Sci. Technol.*, 2012, **7**, (1), 135
67. K. Hou and R. Hughes, *J. Membr. Sci.*, 2002, **206**, (1–2), 119
68. A. Mourgues and J. Sanchez, *J. Membr. Sci.*, 2005, **252**, (1–2), 133
69. S. H. Jung, K. Kusakabe, S. Morooka, S.-D. Kim and J. Membr. Sci., 2000, **170**, (1), 53
70. W. Liang and R. Hughes, *Chem. Eng. J.*, 2005, **112**, (1–3), 81
71. M. Amano, C. Nishimura and M. Komaki, *Mater. Trans. JIM*, 1990, **31**, (5), 404
72. H. Amandusson, L.-G. Ekedahl and H. Dannelun, *Appl. Surf. Sci.*, 2000, **153**, (4), 259
73. A. Li, W. Liang and R. Hughes, *J. Membr. Sci.*, 2000, **165**, (1), 135
74. T. H. Nguyen, S. Mori and M. Suzuki, *Chem. Eng. J.*, 2009, **155**, (1–2), 55
75. S. Hara, K. Sakaki and N. Itoh, *Ind. Eng. Chem. Res.*, 1999, **38**, (12), 4913
76. W.-H. Chen, C.-N. Lin, Y.-H. Chi and Y.-L. Lin, *Int. J. Energy Res.*, 2017, **41**, (11), 1579
77. G. Barbieri, F. Scura, F. Lentini, G. De Luca and E. Drioli, *Sep. Purif. Technol.*, 2008, **61**, (2), 217
78. H. M. Faizal, T. Yokomori and T. Ueda, 'Numerical Investigation on Hydrogen Permeation through Pd/Ag Membrane for H₂/N₂ Mixture Stagnating Flow', 24th International Symposium on Transport Phenomena (ISTP-24), Yamaguchi, Japan, 1st–5th November, 2013
79. E. Nagy, R. Nagy and J. Dudas, *Ind. Eng. Chem. Res.*, 2013, **52**, (31), 10441
80. E. Nagy, *Sep. Purif. Technol.*, 2010, **73**, (2), 194
81. E. Nagy, 'Diffusive Plus Convective Mass Transport Through a Plane Membrane Layer: 5.2 Mass Transport Without Chemical Reaction', "Basic Equation of Mass Transport Through a Membrane Layer", Ch. 5, Elsevier Inc, Amsterdam, The Netherlands, 2012, p. 121
82. F. Gallucci, A. Basile, S. Tosti, A. Iulianelli and E. Drioli, *Int. J. Hydrogen Energy*, 2007, **32**, (9), 1201
83. F. Gallucci, M. De Falco, S. Tosti, L. Marrelli and A. Basile, *Int. J. Hydrogen Energy*, 2008, **33**, (21), 6165
84. F. Gallucci and A. Basile, *Int. J. Hydrogen Energy*, 2006, **31**, (15), 2243
85. W. H. Chen, Y. C. Chung and J. L. Liu, *Int. Commun. Heat Mass Transf.*, 2005, **32**, (5), 695

86. H. M. Faizal, B. B. Nyakuma, M. R. A. Rahman, Md. Mizanur Rahman, N. B. Kamaruzaman and

S. Syahrullail, *Johnson Matthey Technol. Rev.*, 2021, **65**, (1), 77

The Authors



Mohd Faizal Hasan currently is working at the Faculty of Engineering, Universiti Teknologi Malaysia (UTM). He obtained his PhD degree in Engineering from Keio University, Japan. He is actively doing research on densification, torrefaction and gasification of palm biomass, characteristics of hydrogen permeation through palladium/silver purification membranes for fuel cell applications and methanol steam reforming for hydrogen production. In addition to research activities, he is currently teaching Thermodynamics and Applied Thermodynamics.



Bemgba B. Nyakuma obtained his doctoral degree from UTM and currently works at the School of Chemical and Energy Engineering, UTM Skudai Campus, Johor Bahru, Malaysia. He is actively doing research and producing articles in biomass and coal related pretreatment, conversion and utilisation technologies.



Mohd Rosdzimin Abdul Rahman currently is working at the Faculty of Engineering, Universiti Pertahanan Nasional Malaysia. He obtained his PhD degree in Engineering from Keio University, Japan. He is actively doing research on thermal and reactive fluid dynamics.



Md. Mizanur Rahman obtained his PhD in Mechanical Engineering from Aalto University School of Engineering, Finland; MSc in Sustainable Energy Engineering from Royal Institute of Technology (KTH), Sweden; and BSc in Mechanical Engineering from Khulna University of Engineering and Technology, Bangladesh. His research interests include energy economics, renewable energy technologies, biomass digestion and gasification, multicriteria-based rural electrification, energy policy, modelling and optimisation and sustainable energy systems.



Natrah Kamaruzaman obtained her undergraduate level degree from University of The Ryukyus, Japan. Then she obtained Master and Doctoral Degrees from UTM. Currently, she is specialising in microelectronic cooling and heat transfer. Her research interests are focusing on heat transfer, computational fluid dynamics, fluid flow and microchannel and microneedle areas.



Syahrullail Samion is currently working at the Faculty of Engineering, UTM. He obtained his undergraduate, master and doctoral degrees from Kagoshima University, Japan. His areas of expertise are tribology in metal forming, friction and wear tests (tribotester), biolubricants, palm oil as lubricant and fluid mechanics. He is also teaching mechanics of fluids (undergraduate course) and research methodology (master course).